The origin and maintenance of mammalian peroxisomes involves a de novo PEX16-dependent pathway from the ER

Peter K. Kim,[1] Robert T. Mullen,[2] Uwe Schumann,[2] and Jennifer Lippincott-Schwartz[1]

[1]Cell Biology and Metabolism Branch, National Institute of Child Health and Human Development, National Institutes of Health, Bethesda, MD 20892
[2]Department of Cellular and Molecular Biology, University of Guelph, Guelph, Ontario N1G 2W1, Canada

Peroxisomes are ubiquitous organelles that proliferate under different physiological conditions and can form de novo in cells that lack them. The endoplasmic reticulum (ER) has been shown to be the source of peroxisomes in yeast and plant cells. It remains unclear, however, whether the ER has a similar role in mammalian cells and whether peroxisome division or outgrowth from the ER maintains peroxisomes in growing cells. We use a new in cellula pulse-chase imaging protocol with photoactivatable GFP to investigate the mechanism underlying the biogenesis of mammalian peroxisomes. We provide direct evidence that peroxisomes can arise de novo from the ER in both normal and peroxisome-less mutant cells. We further show that PEX16 regulates this process by being cotranslationally inserted into the ER and serving to recruit other peroxisomal membrane proteins to membranes. Finally, we demonstrate that the increase in peroxisome number in growing wild-type cells results primarily from new peroxisomes derived from the ER rather than by division of preexisting peroxisomes.

Introduction

Peroxisomes are small membrane-bound organelles that function in cellular metabolism in diverse ways, including the β- and α-oxidation of fatty acids, the oxidation of bile acids and cholesterol, and conversion of hydrogen peroxide to nontoxic forms. The peroxisome's importance in lipid metabolism and defense against oxidative stress explains why defects in peroxisome biogenesis underlie several severe inherited diseases known as peroxisomal biogenesis disorders, including Zellweger syndrome, infantile Refsum disease, and neonatal adrenoleukodystrophy (Wanders, 2004).

Genetic and proteomic studies in yeast and mammalian cell systems have led to the identification of up to 32 proteins (collectively called peroxins or PEX) involved in peroxisome biogenesis. Of these peroxins, three in mammalian cells—PEX3, PEX16, and PEX19—and two in yeast cells—Pex3p and Pex19p—are specifically involved in peroxisomal membrane protein (PMP) import (Schliebs and Kunau, 2004; for review see Heiland and Erdmann, 2005). When any of these proteins are absent or mutated in cells, peroxisomes disappear. PEX19, a farnesylated protein found in both cytosol and peroxisomes, binds nascent PMPs in the cytoplasm and targets them to the peroxisomal membrane (Jones et al., 2004). PEX3, an integral membrane protein, acts as a docking receptor for incoming complexes of PEX19 and its PMP cargoes (Fang et al., 2004). PEX16, an integral membrane protein absent in most yeast, is thought to serve as a receptor for PEX3 or as a component of the membrane translocator (Honsho et al., 2002; Fang et al., 2004).

Despite knowledge of the essential components involved in peroxisome biogenesis, the origin of peroxisomes has been controversial. The long-standing view is that peroxisomes are semiautonomous organelles, like mitochondria and chloroplasts, which multiply strictly by growth and division (Lazarow and Fujiki 1985; for review see Heiland and Erdmann, 2005). This view is based on the premise that peroxisomal proteins (both matrix and membrane associated) are synthesized on free ribosomes and are imported directly into peroxisomes from the cytoplasm (Lazarow, 2003). However, unlike mitochondria and chloroplasts, peroxisomes can disappear from a cell and be regenerated de novo. For example, cells defective in PEX3, PEX16, or PEX19 do not have any detectable peroxisomes; yet, upon introduction of the wild-type version of the missing or

Correspondence to Jennifer Lippincott-Schwartz: jlippin@helix.nih.gov

U. Schumann's present address is Section of Molecular Biology, Division of Biological Sciences, University of California San Diego, La Jolla, CA 92093.

Abbreviations used in this paper: Cb_5-glyc, cytochrome b_5; FLIP, fluorescence loss in photobleaching; PAGFP, photoactivatable GFP; PBD, peroxisome biogenesis disorder; PMP, peroxisomal membrane protein; PPL, preprolactin; RFP, red fluorescent protein; ROI, region of interest.

The online version of this article contains supplemental material.

The Journal of Cell Biology, Vol. 173, No. 4, May 22, 2006 521–532
http://www.jcb.org/cgi/doi/10.1083/jcb.200601036

mutated gene, peroxisomes are quickly regenerated (South and Gould, 1999; Honsho et al., 2002). This capacity of peroxisomes to regenerate, together with other observations related to the intracellular sorting pathways of PMPs (see the following paragraph), has led to an alternative view of peroxisomal biogenesis, in which other organelles—specifically, the ER—participate in the formation and maintenance of peroxisomal membranes (for reviews see Heiland and Erdmann, 2005; Kunau, 2005; Schekman, 2005).

Several lines of experimental support for an ER-dependent mode of peroxisome biogenesis, especially in yeast and plants, have been obtained over the past few years. For example, in the yeast cell type *Yarrowia lipolytica*, Pex16p and Pex2p are *N*-glycosylated (a modification only occurring in the ER), suggesting they pass through the ER en route to peroxisomes (Titorenko and Rachubinski, 1998). In plant cells, both *Arabidopsis thaliana* Pex16p and cottonseed peroxisomal ascorbate peroxidase localize to a distinct subdomain of the ER called peroxisomal ER in addition to being found in peroxisomes (Mullen et al., 1999; Karnik and Trelease, 2005). Finally, in *Saccharomyces cerevisiae* cells, peroxisomes reappear by outgrowth of Pex3-GFP–containing structures from the ER during complementation of ΔPex3p mutants with Pex3p-GFP (Hoepfner et al., 2005; Tam et al., 2005). In addition, Pex3p that is targeted to the ER by an attached signal sequence is routed to peroxisomes (Kragt et al., 2005). In yeast and plant cells, therefore, the ER seems to play a direct role in delivering lipid and protein components to peroxisomes.

Whether the ER plays a similar role in peroxisome biogenesis in mammalian cells remains unclear. The only evidence suggesting this comes from studies in mouse dendritic cells, in which PEX13 and PMP70 have been reported in reticular structures apparently connected to smooth ER (Geuze et al., 2003). Other studies have provided results that are inconsistent with an ER role. Exogenously expressed PEX3 or PEX19, for example, are not localized to the ER in mammalian cells, even when they are overexpressed in peroxisome-deficient cells (Fang et al., 2004). Because PEX3 does not directly target to the ER in mammalian cells or in plant cells (Hunt and Trelease, 2004), the findings in *S. cerevisiae* related to Pex3p trafficking (and potentially its conclusions regarding the role of the ER in peroxisome biogenesis) may not be generalizable to all organisms. Indeed, peroxisome biogenesis in mammalian cells is widely assumed to occur primarily by fission of preexisting peroxisomes with any de novo pathway, either ER dependent or independent (for reviews see Lazarow, 2003; Yan et al., 2005), occurring only under unusual conditions in mutated cells. The role of the ER in the biogenesis of mammalian peroxisomes would therefore seem to be limited to providing membrane components (e.g., lipids) rather than to providing a platform for the outgrowth of new peroxisomes, as observed in *S. cerevisiae* cells (Hoepfner et al., 2005; Kragt et al., 2005; Tam et al., 2005).

These types of concerns have led us to directly investigate the pathway for peroxisome biogenesis in mammalian cells. Toward this end, we have used monomeric and photoactivated versions of GFP linked to the essential membrane peroxin, PEX16, to address whether specific peroxisomal membrane components in mammalian cells are normally derived from the ER or whether this occurs only when preexisting peroxisomes are missing. We furthermore have used a novel photo-chase strategy highlighting old and new peroxisomes to address whether new peroxisomes in mammalian cells form primarily by growth and division of preexisting peroxisomes or by the maturation of new peroxisomes derived from the ER. Our findings provide the first direct evidence in mammalian cells that the ER plays a central role in both the origin and maintenance of peroxisomes.

Results

PEX16 localizes to peroxisomes and ER and is not present in cytosol

To characterize the dynamic distribution of human PEX16, the COOH terminus of PEX16 was tagged with monomeric versions of various fluorescent proteins (GFP, photoactivatable GFP [PAGFP], or Venus). Two lines of evidence suggested that all of the resulting chimeras targeted and functioned properly when expressed in mammalian cells. First, when PEX16 tagged with GFP (PEX16-GFP) was expressed in COS-7 cells, complete colocalization was observed between PEX16-GFP and a coexpressed peroxisomal reporter molecule consisting of the red fluorescent protein (RFP) tagged to type 1 peroxisomal matrix targeting signal, SKL-COOH (RFP-SKL; Fig. 1 A). Second, in cells from the human fibroblast cell line GM06231 lacking peroxisomes because of a mutated PEX16 gene, introduction of PEX16-GFP led to the appearance of new peroxisomes (Brocard et al., 2005), indicating PEX16-GFP can complement PEX16 function.

COS-7 cells expressing PEX16-GFP at higher levels, achieved by increasing the time between cell transfection and imaging (from 15 to 24 h; Fig. S1, available at http://www.jcb.org/cgi/content/full/jcb.200601036/DC1), were examined to determine whether PEX16-GFP changed its distribution once the machinery involved in PEX16 sorting to peroxisomes became limited by PEX16 overexpression. To identify peroxisomes as well as ER in these cells, the peroxisomal marker RFP-SKL and the ER marker ssRFP-KDEL were individually coexpressed with PEX16-GFP. The distribution of PEX16-GFP in these cells included the ER as well as peroxisomes (Fig. 1 C). Hence, the membrane localization of PEX16-GFP is not restricted to peroxisomes but includes the ER under conditions of high PEX16-GFP expression.

Expression of PEX16-GFP at low levels in the peroxisome biogenesis disorder (PBD) 399-T1 human fibroblast cell line that lacks PEX19 and in which peroxisomes are absent (Sacksteder et al., 2000) showed the chimera residing exclusively in the ER, with RFP-SKL diffusely distributed throughout the cytosol (Fig. 1 E). A similar ER pattern was observed for PEX16-GFP expressed in a PEX3 mutant human fibroblast cell line (PBD400) that, similar to PBD399-T1 cells, lacks peroxisomes (South et al., 2000; unpublished data). When peroxisomes are absent, therefore, PEX16-GFP targets to the ER and not to the cytosol. Cell fractionation and immunoblot analysis of PEX16-GFP–transformed COS-7 cells performed 24 h after transfection to allow for protein overexpression revealed that

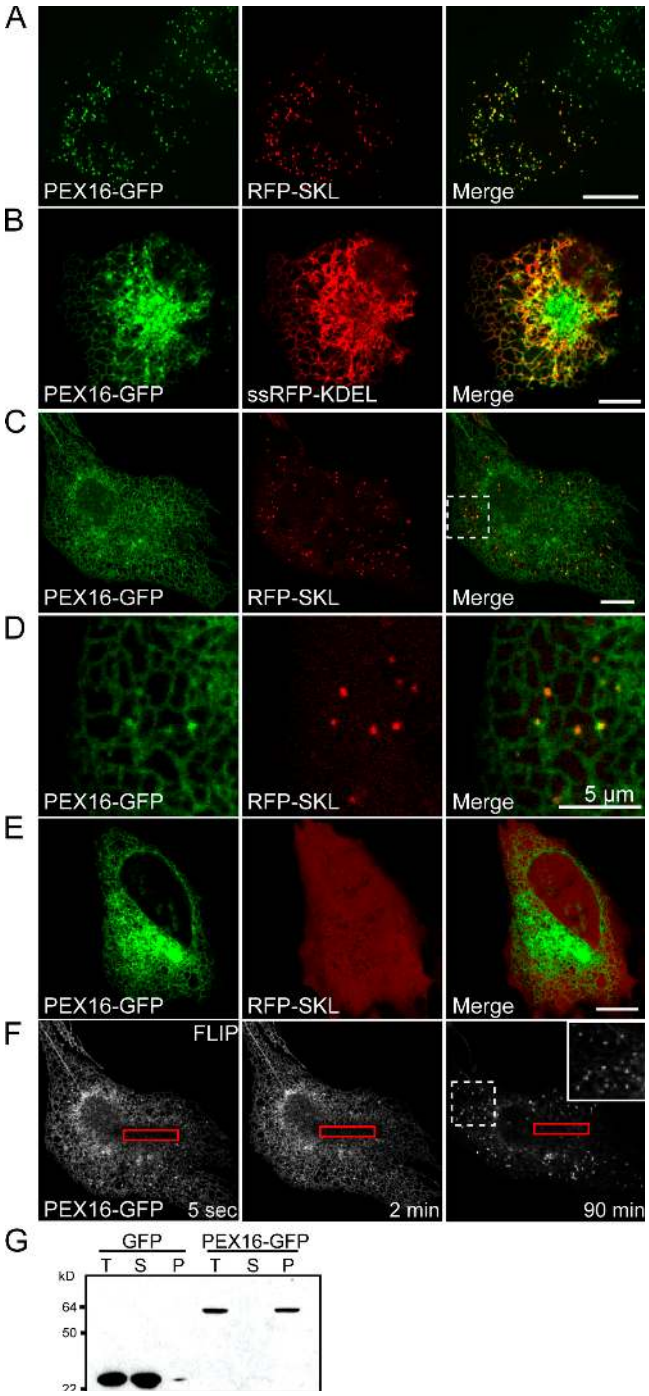

Figure 1. **PEX16-GFP localizes to both peroxisomes and ER.** (A) COS-7 cells transiently coexpressing PEX16-GFP and RFP-SKL imaged 15 h after transfection. (B) COS-7 cells coexpressing PEX16-GFP and ssRFP-KDEL imaged 24 h after transfection. (C) Same as A except the cells were imaged 24 h after transfection. (D) Enlargement of the region outlined by the stripped box in C. Note that PEX16-GFP and RFP-SKL–containing peroxisomes are in close proximity to the ER. (E) PBD399-T1 cell transiently coexpressing PEX16-GFP and RFP-SKL imaged 24 h after transfection. (F) FLIP of the cell shown in C reveals that PEX16-GFP is highly mobile in the ER. The red box outlines the ROI that was subjected to photobleaching with 488-nm laser light. The dotted box (enlarged in inset) shows that PEX16-GFP fluorescence in peroxisomes was unaffected by FLIP, in contrast to PEX16-GFP fluorescence in the ER. (G) Immunoblots of cell fractions from COS-7 cells transiently expressing either GFP or PEX16-GFP. The soluble (S), membrane (P), and prefractionated (T) samples were analyzed by SDS-PAGE/immunoblotting using mouse anti-GFP and goat anti–mouse HRP. Bars: (A–C and E) 10 μm; (D) 5 μm.

PEX16-GFP resided only in the membrane (or nonsoluble fraction), in contrast to GFP expressed alone, which was primarily in the soluble fraction (Fig. 1 G). Hence, PEX16-GFP does not appear to ever reside in the cytosol.

Peroxisomes that were observed in cells having high PEX16-GFP expression were closely aligned with the ER (Fig. 1 C [box] and D), suggesting that peroxisomes and the ER are intimately associated. Repetitive photobleaching (or fluorescence loss in photobleaching [FLIP]) of PEX16-GFP fluorescence in a small, centralized area of the ER in these cells (Fig. 1 F, red box) resulted in PEX16-GFP fluorescence being lost throughout the ER without affecting PEX16-GFP fluorescence in surrounding peroxisomes (Fig. 1 F). Molecules of PEX16-GFP can thus freely diffuse throughout the ER, whereas they are retained within individual peroxisomes.

Photoactivated PEX16-PAGFP moves from the ER to peroxisomes

To investigate whether the ER localization of PEX16 represented an intermediate in the pathway for delivery of PEX16 to peroxisomes, we developed a photo/pulse-chase–labeling assay using PEX16 attached to PAGFP (PEX16-PAGFP). PAGFP is undetected until "activated" by high-energy light, whereupon it becomes brightly fluorescent. Activated PAGFP molecules remain fluorescent over time, whereas PAGFP molecules that have not been photoactivated (including newly synthesized and newly folded forms) stay invisible (Patterson and Lippincott-Schwartz, 2002).

The photo/pulse-chase assay was performed in COS-7 cells coexpressing PEX16-PAGFP and RFP-SKL 24 h after transfection, as outlined in Fig. 2 A. Initially, a small region of interest (ROI; Fig. 2 A, red box) containing only ER (blue) and no peroxisomes (red) was repeatedly irradiated over 30 min with 413-nm light (pre-PA). Because PEX16-GFP diffuses freely throughout the ER, most PEX16-PAGFP molecules in the ER should become photoactivated (Fig. 2 A, green) under this treatment. An image of the cell was collected sequentially in the 543-nm channel to visualize peroxisomes containing RFP-SKL immediately before and after each photoactivation to ensure no peroxisomes moved into the ROI and that no PEX16-PAGFP molecules within peroxisomes become photoactivated. After photoactivation in this manner for 30 min, images of PEX16-PAGFP at 488-nm fluorescence and RFP-SKL at 543-nm fluorescence were acquired (Fig. 2 A, Post-PA t = 0 min). The cell was then incubated for 5 h (chase) before acquiring another set of images (Fig. 2 A, Post-PA t = 5 h) to assess whether fluorescent PEX16-PAGFP molecules had redistributed to RFP-SKL–containing peroxisomes.

As shown in Fig. 2 B, before photoactivation of the ER pool of PEX16-PAGFP, GFP fluorescence (excited at 488 nm) was negligible, whereas the fluorescence attributable to RFP-SKL (543 nm) was readily visible and localized primarily to individual (punctate) peroxisomes (Fig. 2 B, Pre-PA). Upon repeated photoactivation of the small ROI in the lower left part of the cell, PEX16-PAGFP fluorescence became visible in the ER and in a few puncta that partially overlapped with RFP-SKL, suggesting they were peroxisomes (Fig. 2 B, Post-PA

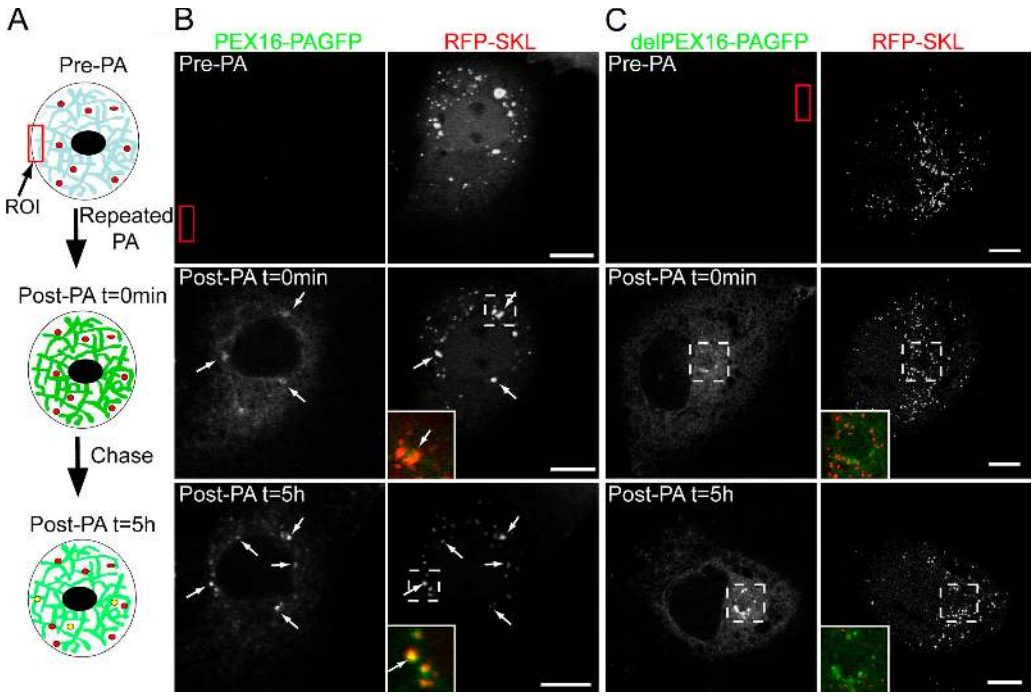

Figure 2. **Photo/pulse-chase assay indicates that PEX16-PAGFP, but not delPEX16-GFP, sorts from the ER to peroxisomes.** (A) Schematic diagram of the photo/pulse-chase assay. (B) Photo/pulse-chase assay performed in COS-7 cell coexpressing PEX16-PAGFP and RFP-SKL. To ensure that all newly synthesized PEX16-PAGFP molecules had time to correctly fold and target to membranes, the cells were treated with 100 μM puromycin before photoactivation. The red box indicates the ROI. Arrows indicates examples of obvious colocalizations of PEX16-PAGFP and RFP-SKL. The insets display the corresponding merged images of coexpressed PEX16-PAGFP (green) and RFP-SKL (red). (C) Photo/pulse-chase assay was performed as described in B, except cells were coexpressing delPEX16-PAGFP and RFP-SKL. Insets represent enlarged merged images of the dotted boxes showing the localization of delPEX16-PAGFP (green) and RFP-SKL (red). Bars, 10 μm.

t = 0 min, arrows). After the 5-h chase period, significantly more PEX16-PAGFP fluorescence was localized in peroxisomes (Fig. 2 B, Post-PA t = 5 h, arrows). Quantification of peroxisomes containing both PEX16-PAGFP and RFP-SKL over the 5-h chase period in five independent experiments revealed that 10–40% of all peroxisomes in these cells became labeled with photoactivated PEX16-PAGFP (unpublished data). Because PEX16-PAGFP molecules were pulse-labeled in the ER and later appeared in peroxisomes, the data suggested that PEX16-PAGFP undergoes specific transport from the ER to peroxisomes.

PEX16 movement from ER to peroxisomes depends on sequences in its NH_2 terminus

To investigate what molecular features of PEX16 were necessary for it to pass from the ER to peroxisomes, we used a PAGFP-tagged variant of PEX16 in which the NH_2-terminal membrane peroxisome–targeting sequence (residues 66–81; -RKELRKK-LPVSLSQQK-; Honsho et al., 2002) was deleted. Expression of this construct (delPEX16-PAGFP) in COS-7 cells resulted in only an ER pattern of localization with no peroxisome labeling (Fig. S2, available at http://www.jcb.org/cgi/content/full/jcb.200601036/DC1). In the photo-chase assay, photoactivation of the ER pool of a cell expressing delPEX16-PAGFP resulted in the fluorescence attributable to delPEX16-PAGFP never redistributing to peroxisomes and remaining within the ER (Fig. 2 C). The small structures containing photoactivated delPEX16-PAGFP seen in the juxtanuclear region of these cells (Fig. 2 C, Post-PA t = 0 min and Post-PA t = 5 h) presumably represented compacted ER cisternae, as their fluorescence was diminished upon repeated photobleaching of a small area of ER in delPEX16-GFP–expressing cells (Fig. S2). Thus, delivery of PEX16 from ER to peroxisomes is dependent on the membrane peroxisome–targeting sequence found within PEX16.

PEX16 with an appended NH_2-terminal type I signal anchor sequence targets to peroxisomes after being synthesized in the ER

Nascent polypeptides containing an NH_2-terminal signal sequence are bound by the signal recognition particle in the cytoplasm and transferred to the ER before the remainder of their mRNA is translated (Rapoport et al., 1996). By attaching such a sequence to the NH_2 terminus of PEX16, we reasoned that we could force newly synthesized PEX16 proteins to be cotranslationally inserted into the ER before they targeted elsewhere in the cell (such as to peroxisomes). With such a construct, we could then address whether PEX16 could target to peroxisomes after being cotranslationally synthesized in the ER. We appended residues 14–90 from the well-defined type I signal anchor sequence of leader peptidase (designated as sa; Gafvelin et al., 1997; Heinrich et al., 2000) to the NH_2 terminus of PEX16-GFP (yielding saPEX16-GFP) to preserve the native (N_{out}-C_{out}; Fig. 3 A) membrane topology of PEX16 (Honsho et al., 2002).

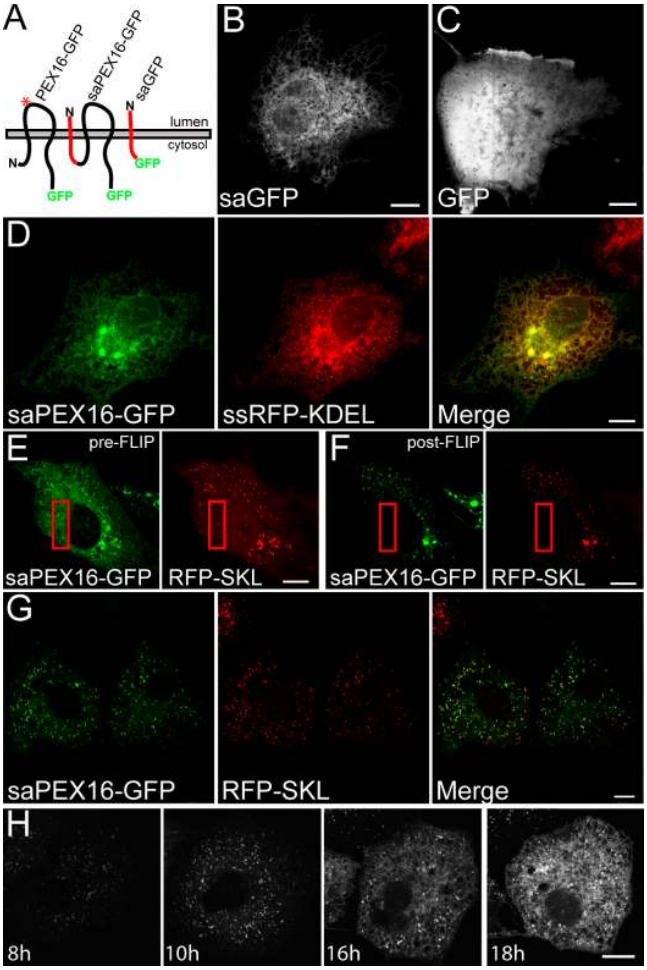

Figure 3. **PEX16 containing an NH_2-terminal signal-anchor sequence localizes to both peroxisomes and ER.** (A) Illustration of the predicted topologies of PEX16-GFP, saPEX16-GFP, and saGFP. sa sequences are shown in red, PEX16 in black, and GFP in green. The asterisk indicates the approximate location of the glycosylation site engineered in PEX16-glyc. (B and C) Images of COS-7 cells transiently transfected with either saGFP (B) or GFP (C) after treatment with 5 μg/ml brefeldin A to block export of proteins from the ER. (D) COS-7 cell coexpressing saPEX16-GFP and ssRFP-KDEL imaged 15 h after transfection. (E and F) Cells coexpressing saPEX16-GFP and RFP-SKL before (E) and after (F) FLIP with 488-nm laser light. (G) Same as E except cells were imaged 8 h after transfection. (H) Time-lapse images of cells expressing saPEX16-GFP at 8, 10, 16, and 18 h after transfection. Bars, 10 μm.

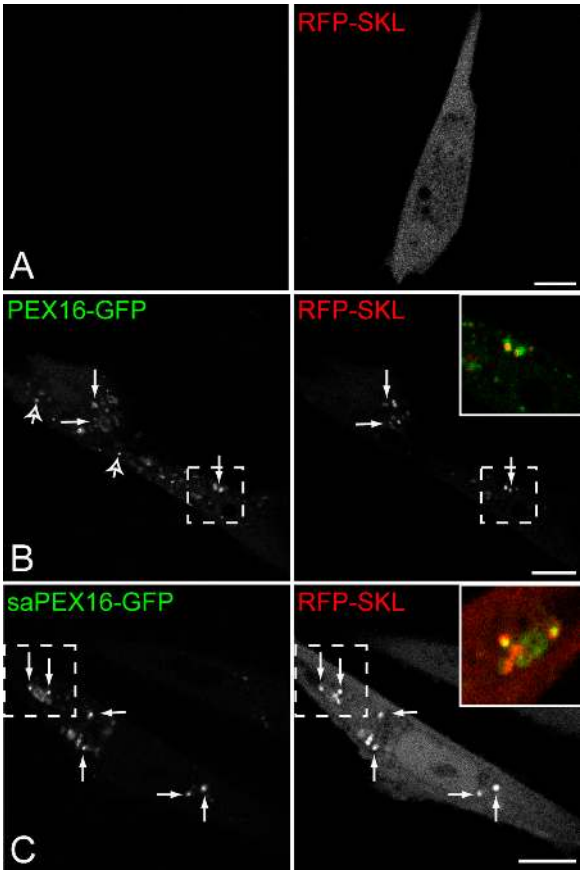

Figure 4. **saPEX16- and PEX16-GFP rescue PEX16-deficient GM06231 cells.** (A–C) GM06231 cells were transiently transfected with pRFP-SKL alone (A) or cotransfected with RFP-SKL and either PEX16-GFP (B) or saPEX16-GFP (C). Live cells were imaged 48 h after transfection. The solid arrows in B and C indicate colocalization between the GFP and RFP signals. The open arrows indicate punctate structures containing either PEX16- or saPEX16-GFP only. The insets show enlarged portions of the cells outlined by dotted boxes. (left) Images excited at 488 nm; (right) images excited at 543 nm. Bars, 10 μm.

Evidence that sa functioned properly as a signal sequence for targeting of proteins to the ER was demonstrated by appending it to GFP alone (producing saGFP) and expressing the construct in COS-7 cells treated with brefeldin A to block secretory transport out of the ER. In these cells, saGFP accumulated in the ER (Fig. 3 B), whereas untagged GFP expressed in COS-7 cells was distributed diffusely throughout the cytosol and nucleus (Fig. 3 C).

To test whether saPEX16-GFP could target to peroxisomes after biosynthesis in the ER, we examined COS-7 cells coexpressing saPEX16-GFP and ssRFP-KDEL 15 h after transfection. A large pool of saPEX16-GFP could be seen colocalized with ssRFP-KDEL in the ER (Fig. 3 D). Differential permeabilization and antibody binding experiments demonstrated that saPEX16-GFP in the ER maintained the same C_{out} topology as that of PEX16-GFP (Fig. S3, available at http://www.jcb.org/cgi/content/full/jcb.200601036/DC1). Repetitive photobleaching (i.e., FLIP) of saPEX16-GFP fluorescence in an area of ER abolished saPEX16-GFP fluorescence throughout the ER and revealed a pool of saPEX16-GFP fluorescence in peroxisomes (Fig. 3, E and F; note the localization of saPEX16-GFP– in RFP-SKL–containing peroxisomes in Fig. 3 F). Therefore, saPEX16-GFP can undergo transport to peroxisomes after being synthesized in the ER.

When the cells were imaged at earlier times after transfection (8 h) to examine saPEX16-GFP localization at lower expression levels, saPEX16-GFP was exclusively colocalized with RFP-SKL in peroxisomes (Fig. 3 G). A possible explanation for this is that saPEX16-GFP moves efficiently from ER to peroxisomes until excess saPEX16-GFP saturates the machinery for targeting to peroxisomes. Consistent with this, time-lapse imaging of cells expressing saPEX16-GFP over a 10-h period (during which saPEX16-GFP expression levels went from low to high) revealed newly synthesized saPEX16-GFP accumulating in peroxisomes before also accumulating in the ER (Fig. 3 H).

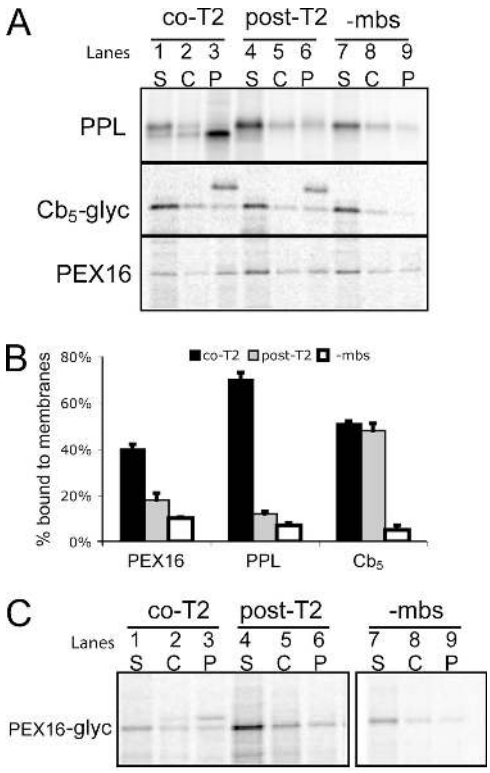

Figure 5. **PEX16 targets cotranslationally to ER in vitro.** (A) Autoradiographs of the in vitro ER microsome binding assays with PPL (~30 kD), Cb_5-glyc (~20 kD), and PEX16 (~37 kD) in both cotranslational (co-T2) targeting and posttranslational (post-T2) conditions. Lanes represents fractions from membrane pelleting over a sucrose cushion. The lower molecular mass band in lane 3 for PPL is due to the processing of the PPL's cleavable signal sequence. The higher molecular mass band in lanes 3 and 6 for Cb_5-glyc is due to its N-linked glycosylation. −mbs, no ER microsomes; S, supernatant; C, cushion; P, pellet. (B) Representative histograms illustrating the percentage of total protein accumulated in the pellet after either co-T2 or post-T2 targeting or when no ER microsomes were included in the binding assays. Error bars indicate one standard deviation. $n = 3$. (C) In vitro ER microsome binding assays with PEX16-glyc. Procedures similar to those in A were followed; however, pelleted membranes were washed with 0.5 M KOAc and 50 mM EDTA after centrifugation. The higher molecular mass band in lane 3 represents glycosylated PEX16-glyc protein in the pelleted ER microsomes.

PEX16 with a signal anchor sequence complements wild-type PEX16 in cells lacking the *PEX16* gene

To determine whether saPEX16-GFP could complement PEX16 function and give rise to new peroxisomes, cells from the human GM06231 cell line lacking peroxisomes were transfected with RFP-SKL, PEX16-GFP and RFP-SKL, or saPEX16-GFP and RFP-SKL. The distribution of GFP and/or RFP fluorescence in these cells was then examined 48 h after transfection (Fig. 4). In cells transfected with RFP-SKL alone, the peroxisomal reporter was distributed diffusely in the cytosol and no fluorescence at 488 nm was detected, indicating that peroxisomes were indeed absent in these cells (Fig. 4 A). In contrast, in cells cotransfected either with PEX16-GFP and RFP-SKL (Fig. 4 B) or with saPEX16-GFP and RFP-SKL (Fig. 4 C), numerous punctate and globular peroxisomal structures containing both sets of expressed proteins were observed (Fig. 4, B and C, arrows). Because the signal anchor sequence on saPEX16-GFP forced it to be inserted into the ER membrane before delivery to other membranes, these results indicated that a pathway from the ER involving PEX16 was sufficient to support peroxisome production de novo.

Interestingly, some of the punctate structures in the cells coexpressing the GFP-tagged PEX16 and RFP-SKL molecules contained only PEX16- or saPEX16-GFP. These structures may represent so-called early or nascent peroxisomes (South and Gould, 1999; Honsho et al., 2002) that have not yet begun importing lumenal peroxisomal proteins after *PEX16* complementation.

Wild-type PEX16 inserts into ER membranes in a cotranslational, rather than posttranslational, manner in vitro

There are two ways in which wild-type nascent PEX16 can target to the ER: (1) by posttranslational targeting, in which PEX16 is synthesized on free ribosomes in the cytoplasm and then is posttranslationally targeted to and inserted into ER membranes, or (2) by cotranslational targeting, in which ribosomes containing NH_2-terminal PEX16-nascent chains are first targeted to the ER and then PEX16 is cotranslationally inserted into ER membranes. To distinguish between these two possibilities, we used an in vitro binding assay in which PEX16 was synthesized using a rabbit reticulocyte lysate in the presences of ^{35}S-methionine. To assay for cotranslational targeting, the translation reaction was performed in the presence of ER microsomes. To assay for posttranslational targeting, ER microsomes were added to the reaction after the protein was first fully translated and further protein translation was inhibited by the addition of cycloheximide. Preprolactin (PPL) and cytochrome b_5-glyc (Cb_5-glyc; cytochrome b_5 with a glycosylation site in its luminal domain) were used as appropriate cotranslation and posttranslation controls, respectively (Andrews et al., 1989; Pedrazzini et al., 2000).

As shown in Fig. 5 (A and B), PEX16 pelleted more readily with ER microsomes during cotranslational targeting (39%) than during posttranslational targeting (18%) or during translation without microsomes (10%). These results were similar to those observed for the cotranslational targeting of PPL; i.e., significantly more PPL pelleted with microsomes with its signal sequence cleaved during co-T2 targeting compared to post-T2 targeting (Fig. 5 A [PPL, compare lane 3 with 6 and 9] and B). In contrast, Cb_5-glyc exhibited binding to ER microsomes both when microsomes were added during the translation reaction and when microsomes were added after translation (Fig. 5 A, Cb_5-glyc), as expected for this posttranslationally targeted protein (Pedrazzini et al., 2000). Furthermore, the actual integration of Cb_5-glyc into ER microsomes was demonstrated by its glycosylation, which shifted it to a higher molecular mass in the pellet fraction (Fig. 5 A, lanes 3 and 6).

The increase of PEX16 in the pellet fraction during posttranslational targeting experiments compared with minus membrane experiments (Fig. 5, A and B) may be due to nonspecific interactions of PEX16's hydrophobic transmembrane domains with microsomes rather than to PEX16's actual integration into the lipid bilayer of the ER. To determine whether

this was the case, we engineered a glycosylation site at the putative luminal domain of PEX16 (PEX16-glyc; N-X-S starting at residue 161; Fig. 3 A). We reasoned that if any PEX16-glyc molecules in the assay were glycosylated, they must have been specifically integrated into ER microsomes. As shown in Fig. 5 C, a significant proportion of PEX16-glyc molecules underwent glycosylation during cotranslational targeting, whereas none did so during posttranslational targeting. The data thus confirmed that PEX16 undergoes cotranslational insertion into the ER under in vitro conditions.

PEX16 can recruit other PMPs to the ER

It was previously hypothesized that PEX16 acts as part of the machinery involved in recruiting PMPs to membranes (Honsho et al., 2002; Fang et al., 2004). If so, overexpressed PEX16 that is localized to the ER should cause other PMPs, such as PEX3 and PMP34, to retarget to ER membranes. To test this prediction, we constructed chimeras of PEX3 and PMP34 fused to the GFP or Cerulean blue fluorescent protein (Rizzo et al., 2004) and examined their subcellular location in the presence or absence of overexpressed PEX16 fused to the Venus fluorescent protein (PEX16-Venus; Nagai et al., 2002).

Neither PEX3- nor PMP34-GFP was targeted to the ER when expressed in cells lacking peroxisomes (Fig. S4, available at http://www.jcb.org/cgi/content/full/jcb.200601036/DC1) or in cells containing peroxisomes (Fig. 6, A, B, D, and E). Indeed, PEX3-GFP was colocalized exclusively with RFP-SKL in peroxisomes at low expression levels (Fig. 6 A) and accumulated in mitochondria at higher expression levels (Fig. 6 B). PMP34-Cerulean was also localized to peroxisomes at low expression levels (Fig. 6 D) but accumulated in the cytoplasm at higher expression levels (Fig. 6 E). Importantly, when PEX16-Venus was coexpressed with either PEX3- or PMP34-Cerulean, both PMPs colocalized with PEX16-Venus in the ER (Fig. 6, C and F). When a small area of the ER was repeatedly photobleached to remove ER fluorescence in cells coexpressing the PMPs and PEX16-Venus, both PMPs were observed in peroxisomes (unpublished data). Similar colocalizations of PEX16-Venus and PEX3-Cerulean in the ER were observed in the PBD399-T1 fibroblast cells lacking peroxisomes (Fig. S4), indicating that the recruitment of PEX3-Cerulean by PEX16-Venus to the ER also occurred in other cells. Hence, PEX16 appears to function in the recruitment of PEX3 and PMP34, and possibly other PMPs, to membranes.

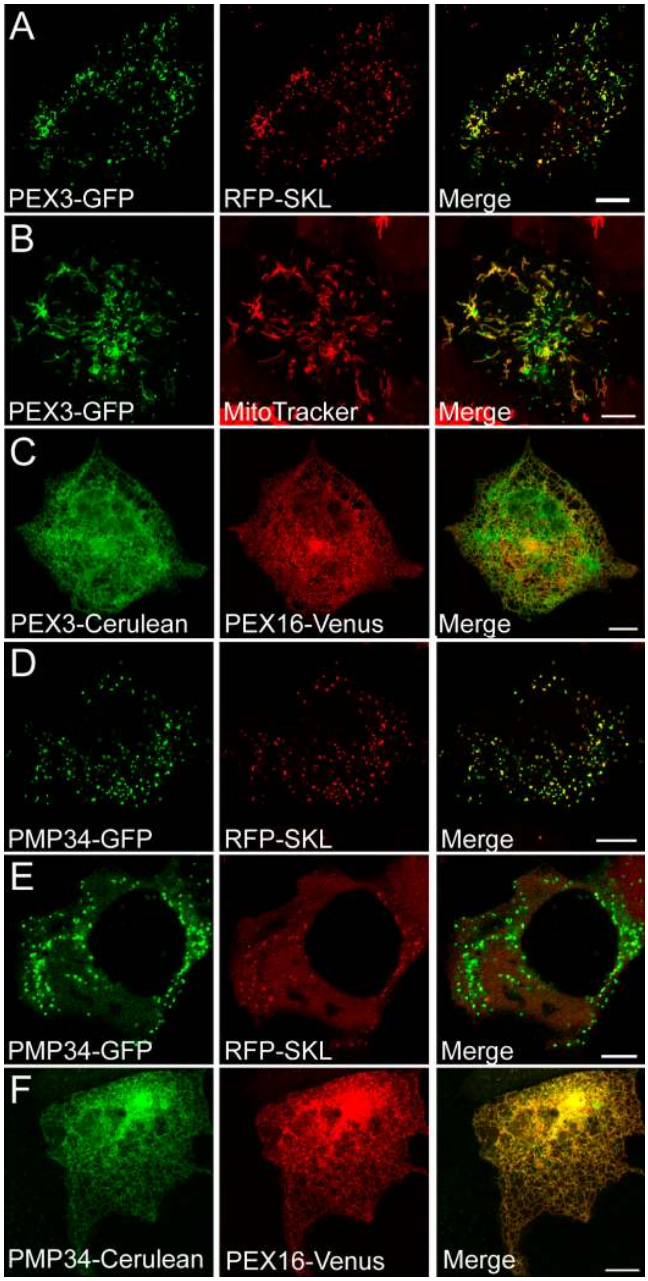

Figure 6. **PEX16 recruits PEX3 and PMP34 to the ER.** (A and B) COS-7 cells either coexpressing PEX3-GFP and pRFP-SKL 15 h after transfection (A) or expressing PEX3-GFP and stained with MitoTracker 24 h after transfection (B). (C) A COS-7 cell expressing PEX16-Venus and PEX3-Cerulean 24 h after transfection. (D and E) COS-7 cells coexpressing PMP34-GFP and RFP-SKL were imaged either 15 h (D) or 48 h (E) after transfection. (F) Cell coexpressing PEX16-Venus and PMP34-Cerulean imaged 24 h after transfection. Bars, 10 μm.

Distinguishing de novo peroxisome biogenesis from peroxisome fission in wild-type cells

Recent studies in *S. cerevisiae* cells have suggested that de novo biogenesis of peroxisomes occurs by direct outgrowth of peroxisomal structures from the ER (Hoepfner et al., 2005; Kragt et al., 2005; Tam et al., 2005). To test whether a similar mechanism occurs in mammalian cells, we devised an assay to directly visualize the formation of peroxisomes in wild-type mammalian cells (Fig. 7 A). The assay involved two photoactivation events separated by 24 h that permitted old and new peroxisomal components to be differentiated in living cells. We reasoned that daughter peroxisomes formed by division of preexisting peroxisomes should all contain peroxisomal components from their mother peroxisomes. However, peroxisomes formed by a de novo pathway from the ER should contain only newly synthesized components. Therefore, by distinguishing recently synthesized peroxisomal components from older peroxisomal components, we could distinguish peroxisomes formed de novo from those formed by fission.

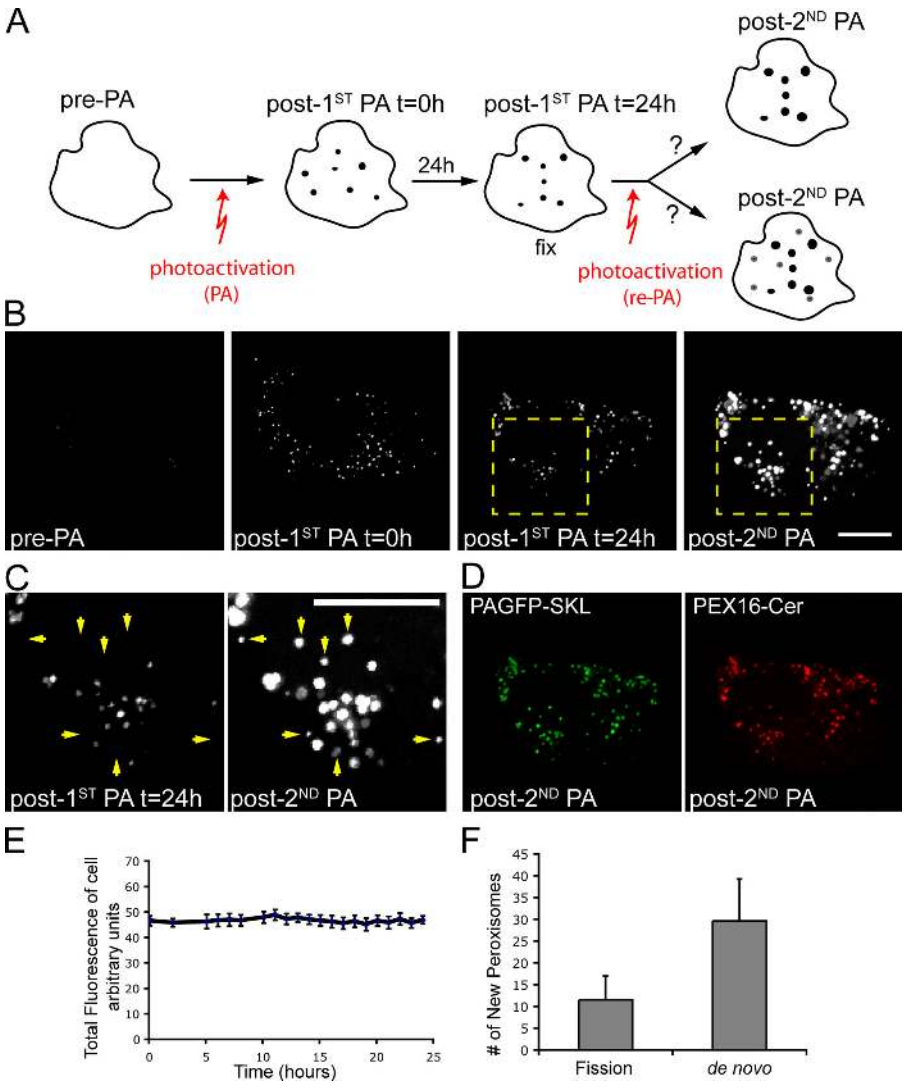

Figure 7. **Peroxisome biogenesis assay.** (A) Schematic representation of the peroxisome photo-chase biogenesis assay. (B) Images of PAGFP-SKL at different time points during the assay. (C) Enlargement of the areas outlined by the stippled boxes in post-1st PA t = 24 h and post-2nd PA in B. Arrows indicate new peroxisomes that were observed only after the second photoactivation event. (D) Distribution of PAGFP-SKL and PEX16-Cerulean after the second photoactivation shows that all of the photoactivated PAGFP-SKL structures contain PEX16-Cerulean. (E) The mean of the total fluorescence intensity (n = 3) attributable to PAGFP-SKL in the PAGFP-SKL/PEX16-Cerulean–expressing NRK cells excited with 488 nm plotted over a 24-h period. Images were collected with a fully open pinhole. The total fluorescence in the cells was calculated by multiplying the mean pixel value of the whole cell with the total number of pixels in the image of the cell. Error bars indicates the standard deviation. n = 3. (F) The mean number of peroxisomes formed by fission versus de novo pathways. The number of new peroxisomes formed by fission was determined by measuring the difference in the number of peroxisomes in the post-1st PA t = 24 h and post-1st PA t = 0 images. The number of peroxisomes formed de novo was determined by measuring the difference between the post-2nd PA and post-1st PA t = 24 h images (see Materials and methods for additional details). The mean number of peroxisomes formed by fission in the 24-h period was calculated as 11 ± 5 (n = 8), whereas a mean of 30 ± 10 (n = 8) new peroxisomes were calculated to be formed de novo. The difference between these two conditions was determined to be statistically significant ($P < 0.05$; paired t test). Bars, 10 μm.

NRK cells were transiently transfected with PAGFP fused to SKL (PAGFP-SKL) to mark preexisting peroxisomes and with PEX16-Cerulean to monitor peroxisomes before (pre-PA) and after (post-1st PA t = 0 h) photoactivation of PAGFP-SKL (Fig. 7 A). All PAGFP-SKL molecules in the peroxisomes of the cell were initially photoactivated using 413-nm laser light, and an image was collected (post-1st PA t = 0 h). The cell was then incubated at 37°C for 24 h to allow newly synthesized, nonphotoactivated PAGFP-SKL molecules to accumulate. The cell was then fixed to prevent peroxisomes from moving, and another image was collected (post-1st PA t = 24 h). Immediately thereafter, the cell was photoactivated a second time (re-PA) to highlight all newly synthesized (previously "invisible") PAGFP-SKL molecules, and a final image was collected (post-2nd PA). The image acquired after the second PA (post-2nd PA) was compared with the previous image (i.e., post-1st PA t = 24 h) to determine whether the PAGFP-SKL molecules that were synthesized during the 24 h were only localized to previously fluorescent peroxisomes or if they were localized to both previously fluorescent peroxisomes and nonfluorescent nascent peroxisomes within in the cell.

Before photoactivation, no fluorescence attributable to PAGFP-SKL was observed in a cell coexpressing PAGFP-SKL and PEX16-Cerulean (Fig. 7 B, pre-PA; and not depicted). However, upon photoactivation, punctate peroxisomes containing PAGFP-SKL became brightly fluorescent (Fig. 7 B, post-1st PA t = 0 h). Imaging of the same cell 24 h later revealed a minimal loss of fluorescent signal in the cell (Fig. 7 B, post-1st PA t = 24 h). Indeed, quantification of the PAGFP-SKL fluorescence in different cells throughout the 24-h period revealed that the level of fluorescence remained virtually constant (Fig. 7 E). This suggested that PAGFP-SKL proteins were long-lived and that repeated low-light imaging did not lead to their fluorescence being photobleached. The number of fluorescent peroxisomes measured at the start and end of this imaging period only slightly increased (~8%), presumably because of peroxisomes undergoing fission (Fig. 7 F, fission).

After the second photoactivation, the fluorescence associated with already fluorescent peroxisomes increased significantly (Fig. 7 B, compare post-1st PA t = 24 h and post-2nd PA). Once formed, therefore, peroxisomes continue to import newly synthesized PAGFP-SKL. Notably, fluorescence also appeared

in peroxisomes that were not previously fluorescent (i.e., peroxisomes that did not contain any PAGFP-SKL molecules highlighted during the first photoactivation step; Fig. 7 B [post-2nd PA] and C [higher magnification, arrows]). These "new" peroxisomes were not the result of preexisting peroxisomes that had lost their fluorescent signal by either degradation or photobleaching after the initial photoactivation, as the total fluorescent signal from photoactivated PAGFP-SKL did not diminish over the 24-h chase period (Fig. 7 E). Rather, they appeared to represent peroxisomes formed de novo during the 24-h chase period.

Quantification of the number of newly appearing peroxisomes after the second photoactivation event was determined by calculating the difference in the number of peroxisomes before and after the second photoactivation. A mean of 30 ± 10 new peroxisomes per cell was found based on results from eight independent experiments (Fig. 7 F). This represented an $\sim$20% increase in the total number of peroxisomes in the cell over the 24-h period and was much greater than the slight increase in peroxisomes observed after the first photoactivation based on a *t* test ($t = 2.42$; $P < 0.05$). Therefore, a de novo pathway appeared to play a significant role in the formation of peroxisomes in these cells.

Discussion

In this study, we provide evidence based on live cell imaging approaches that peroxisomes in mammalian cells can arise de novo from the ER. Using PAGFP and in cellula pulse-chase analysis of PAGFP-labeled PEX16 (an early event peroxin), we demonstrate that PEX16 traffics normally from the ER to peroxisomes and that peroxisomes arise from the ER in wild-type cells and not only in mutant cells lacking peroxisomes. We further show that PEX16 is incorporated into ER-derived microsomes cotranslationally and that PEX16 is capable of recruiting other PMPs to membranes. Finally, by visualizing the production of peroxisomes within a cell over time using PAGFP, we show that most new peroxisomes are derived de novo, with possibly only a minor fraction arising from fission of preexisting organelles.

Our findings complement the growing body of evidence from yeast cells, including *S. cerevisiae* and *Y. lipolytica*, and plant cells indicating that peroxisomes originate from the ER and are not semiautonomous organelles like mitochondria or chloroplasts (Titorenko and Rachubinski, 1998; Mullen et al., 1999; Hoepfner et al., 2005; Karnik and Trelease, 2005; Kragt et al., 2005; Tam et al., 2005). In addition to solidifying this new concept, our results help clarify the role of PEX16 in promoting peroxisome outgrowth from the ER and introduce a new pulse-chase assay using PAGFP in living cells for examining peroxisome biogenesis under various physiological conditions.

ER-dependent peroxisome biogenesis

Several lines of evidence for a role of the ER in peroxisome biogenesis are presented in this study. First, PEX16-GFP in wild-type cells was localized solely in peroxisome and ER membranes with no cytosolic pool and was found only in the ER in peroxisome-less, PEX19 mutant cells (Fig. 1). Second, PEX16 was shown to cotranslationally insert into isolated ER microsomes (Fig. 5), and when it was forced to cotranslationally insert into the ER of live cells through the attachment of a signal sequence, acquired a topological orientation (Fig. S3; N_{out}-C_{out}) similar to that reported for PEX16 in peroxisomal membranes (Honsho et al., 2002). Third, PEX16 could transit from the ER to peroxisomes, indicating that the cotranslational targeting of PEX16 into ER was not the final destination of the protein. This latter conclusion was clearly demonstrated using a variant of PEX16 tagged with PAGFP. When the ER pool of PEX16-PAGFP was photoactivated and followed over time, the photoactivated molecules redistributed to peroxisomes (Fig. 2 B). Delivery of PEX16 to peroxisomes from the ER was also shown to be specific, as photoactivated PEX16 molecules lacking the NH_2-terminal membrane peroxisomal targeting sequence (delPEX16-PAGFP) were not targeted to peroxisomes but instead remained exclusively in the ER (Fig. 2 C). Finally, expression of either PEX16- or saPEX16-GFP (PEX16 containing a signal anchor sequence to ensure its initial membrane integration into the ER) complemented PEX16 function in GM06231 cells (which normally lack peroxisomes) and gave rise to new peroxisomes (Fig. 4).

Peroxisome maturation from the ER in mammalian cells

After its cotranslational targeting to the ER, we envision that PEX16 recruits to ER membranes other peroxisomal components that are essential for peroxisome biogenesis, including PEX3 and other peroxins. These events would then lead to the import of additional peroxisomal proteins and result in the differentiation of a "peroxisome-like" domain in the ER that eventually would detach from the ER and transform, presumably through some type of maturation process, into a nascent mature peroxisome.

Much of our data and those from other studies are consistent with this view. The idea that PEX16 serves as a receptor to recruit peroxisome proteins to membranes (Honsho et al., 2002; Fang et al., 2004) was supported by our finding that expression of PEX16-GFP is sufficient to retarget overexpressed PEX3 and PMP34 to ER from mitochondria and cytosol, respectively (Fig. 6). The differentiation of a peroxisome-like domain in the ER has been suggested by EM findings in mouse dendritic cells in which novel lamellae structures containing peroxisomal membrane components are observed connected to specialized subdomains of the ER (Geuze et al., 2003). Moreover, in peroxisome-deficient *S. cerevisiae* cells lacking the Pex3 gene, peroxisomes emerge from specialized areas of the ER upon complementation with Pex3-GFP (Hoepfner et al., 2005; Kragt et al., 2005; Tam et al., 2005). Finally, new peroxisomes were reported to form by a process that was independent of coated vesicles (i.e., COPI and -II; South et al., 2000). In line with this, we found that photoactivated PEX16-PAGFP in the ER could redistribute to peroxisomes when COPI-coated vesicle formation was blocked with brefeldin A (unpublished data).

Additional work now needs to be done to clarify how such a maturation process for peroxisome biogenesis from the ER

actually occurs. It is possible, for example, that because the dynamin-like protein DLP-1 has been reported to be required for peroxisome fission (Koch et al., 2004), it is likewise involved in the budding of nascent peroxisomes from the ER. The differences in peroxisome import machinery among evolutionarily diverse organisms must also be explained. For instance, whereas Pex3p in yeast cells readily targets to the ER (Hoepfner et al., 2005; Kragt et al., 2005; Tam et al., 2005), PEX3 in mammalian cells and Pex3p in plant cells appear to be incapable of independently targeting to the ER (South et al., 2000; Hunt and Trelease, 2004; Jones et al., 2004). Indeed, PEX3 only targets to the ER in mammalian cells when it is coexpressed with PEX16 (Fig. 6 D), which is absent in *S. cerevisiae* cells (Honsho et al., 2002). Therefore, one possibility is that the cotranslational insertion of PEX16 into mammalian ER provides the initial "seed" or "scaffold" for recruiting other components (e.g., PEX3) that are required for peroxisome biogenesis from the ER. How such a process would occur in *S. cerevisiae* cells needs to be further addressed, as *PEX16* is absent in these cells. *Y. lipolytica* is the only known yeast that expresses a protein, YlPex16p, containing PEX16 homology. Although YlPex16p shares 24% identity to the human PEX16 (Eitzen et al., 1997; South and Gould, 1999), it is unlikely to function like PEX16 as a PMP receptor. This is because YlPex16p is a luminal membrane protein located inside of the organelle, whereas PEX16 is a multispanning membrane protein (Eitzen et al., 1997; Titorenko and Rachubinski, 1998; Honsho et al., 2002). Instead, YlPex16p may serve as a negative regulator of peroxisome division (Guo et al., 2003).

Contribution of de novo biogenesis versus fission in the formation of new peroxisomes in growing mammalian cells

A critical question for an ER-dependent mode of protein delivery to peroxisomes is what role this pathway plays in manufacturing new peroxisomes in normal, constitutively dividing cells in which fission (division) of preexisting peroxisomes is possible. To address this question, we devised a novel photo-labeling, pulse-chase strategy for distinguishing newly synthesized from previously synthesized peroxisomal protein components and for visualizing both "old" and "new" peroxisomes (Fig. 7). We found that old peroxisomes contained both newly synthesized and previously synthesized protein components, whereas new peroxisomes contained only newly synthesized peroxisomal protein components. These findings argued against fission being the sole mechanism for mammalian peroxisome synthesis and indicated that some other mechanism was responsible for the production of new peroxisomes. One possibility is that the new peroxisomes arise from the budding of very small structures out from preexisting peroxisomes, as proposed for *Hansenula polymorpha* yeast peroxisomes (Veenhuis et al., 2000). However, we think this is unlikely because numerous EM studies have failed to observe peroxisome budding from preexisting peroxisomes in mammalian cells (Novikoff and Holtzman 1976; Geuze et al., 2003), and a key peroxisomal membrane import component (PEX16) targets indirectly to peroxisomes via the ER (Fig. 2). Instead, the simplest interpretation of our data is that the newly synthesized peroxisomes arise by a de novo pathway from the ER, with only a minor fraction being formed by fission of preexisting organelles. Our findings thus help solidify the view that peroxisomes are derived from the ER and provide a useful framework for future work aimed at understanding how peroxisome proliferation is regulated in response to drugs or other physiological conditions.

Materials and methods

Cell lines and reagents

COS-7 and NRK cells were obtained from the American Type Culture Collection. The immortalized PEX19-deficient human skin fibroblast cell line PBD399-T1 and the PEX16-deficient human skin fibroblast cell line GM06231 were gifts from S.J. Gould (John Hopkins University School of Medicine, Baltimore, MD) and P.A. Walton (University of Western Ontario, London, Canada), respectively. All cells were cultured in DME (Biosource International) supplemented with 10% heat-inactivated fetal bovine serum (Biosource International) and 2 mM glutamine (Invitrogen) at 37°C in a humidified atmosphere containing 5% CO_2.

Rabbit anti–mouse HRP antibodies (Sigma-Aldrich), mouse anti-GFP IgGs (CLONTECH Laboratories, Inc.), Alexa Fluor 546 goat anti–mouse IgGs, and MitoTracker (Invitrogen) were used according to manufacturers' instructions. Canine pancreatic ER microsomes and rabbit reticulocyte lysate were gifts from R.S. Hegde (National Institutes of Health, Bethesda, MD). All restriction enzymes were purchased from New England Biolabs, Inc.

Plasmids

The construction of pPEX16-GFP was described previously (Brocard et al., 2005). pPEX16-PAGFP and -Venus were generated by excising the *PEX16* ORF from pPEX16-GFP with BglII and SalI and ligating the resulting fragment into the same sites in either pmPAGFP-N1 (Patterson and Lippincott-Schwartz, 2002) or pVenus-N1 (Nagai et al., 2002). pdelPEX16-GFP encoding the *PEX16* ORF lacking its mPTS (residues 66–81; -RKELRKKL-PVSLSQQK-; Honsho et al., 2002) was generated using QuikChange PCR site-directed mutagenesis (Stratagene) with pPEX16-GFP as template DNA and the complementary synthetic oligonucleotides Fp 5′-GCCGCTCAATG-ACGGGATCCTAAAGCTGCTGACATGGCTGAGCG-3′ and Rp 5′-CGCT-CAGCCATGTCAGCAGCTTTAGGATCCCGTCATTGAGCGGC-3′.

The primers Fp 5′-GTGGTACCATGGAGAAGCTGCGG-3′ and Rp 5′-GTCGACTCAGCCCCAACTGTAG-3′ were used to amplify the *PEX16* ORF, which was then ligated into NcoI–SalI–digested pSPUTK (Kim et al., 1997) to yield psUTK-PEX16. psUTK-PEX16-glyc was constructed by site-directed mutagenesis of two sites in the *PEX16* ORF using the primers Fp 5′-CACAGCCCTGGCAACC**GATC**GCAGTCCTACGTGGGG-3′ and Rp 5′-CCCCACGTAGGACTGC**GATC**GGTTGCCAGGGCTGTG-3′. The bolded nucleotides represent mutations that resulted in two amino acid substitutions, H162R and E163S, as well as the introduction of an N-linked glycosylation consensus site (-N-X-S-) at residues 161–163, along with a novel PvuI restriction site for the convenient assessment of mutant clones. pSA1 was a gift from R.S Hedge. psaPEX16-GFP was constructed by amplifying the sequence encoding amino acid residues 14–90 in SA1 from pSA1 with the primers Fp 5′-GATGCTAGCGATGGCAATATGTTTGC-CCTG-3′ and Rp 5′-GTCAGCTCTCTGGTAGATAGGATC-3′. The resulting PCR products were then digested with NheI and BglII and ligated into NheI–BglII–digested pPEX16-GFP.

pPMP34 was a gift from R.J.A. Wanders (University of Amsterdam, Amsterdam, Netherlands; Visser et al., 2002). The *PMP34* ORF was amplified from pPMP34 with the primers Fp 5′-GCTGAATTCCACCATGGCTTCCGTGCT-GTCCT-3′ and Rp 5′-TTCGGATCCCGGTGTTGGTGTGCACGCTTCAGCC-3′, PCR products were digested with EcoRI and BamHI and ligated into equivalent sites within either pmGFP-N1 or pmCeruleanBlue-N1 to yield pPMP34-GFP and -Cerulean, respectively. The pPEX3-GFP and -Cerulean were generated by amplifying the *PEX3* ORF in pCMV-SPORT-PEX3 (MGC-9125; American Type Culture Collection) using the PCR and oligonucleotides Fp 5′-GAAGA-TCTGCCACCATGCTGAGGTCTGTATGGAATT-3′ and Rp 5′-AAAAGTCGA-CTTCTCCAGTTGCTGAGGGGTAC-3′. The resulting products were digested with BglII and SalI and then ligated into equivalent sites in either pmGFP-N1 and pCeruleanBlue-N1. pmRFP- and pPAGFP-SKL were generated using the oligonucleotides Fp 5′-CGGGATCCACCGGTCGCCACCATG-3′ and Rp 5′-CAGCGGCCGCTTAAAGCTTGGAGGCGCCGGTGGAGTGGCG-3′

and either pmRFP-N1 or pmPAGFP-N1 as template DNA. The resulting products were digested with BamHI and NotI and then ligated into pmRFP-N1. All plasmids were confirmed by automated sequencing. The plasmid pssRFP-KDEL (encoding for an RFP molecule containing a signal sequence of PPL to target it to the ER lumen and a KDEL sequence to retain it there) was a gift from E.L. Snapp (Albert Einstein College of Medicine, Bronx, NY).

Cell culturing and sample preparation for microscopy

In preparation for transient transfections, cells were grown in four-well, Lab-Tek chambered coverglasses to 70–80% confluency. Transient transfections of COS-7 and NRK cells were performed using FuGENE 6 according to the manufacturer's instructions (Roche Molecular Biochemicals). The Lipofectamine 2000 transfection reagent (Invitrogen) was used for PBD399-T1 and G062351 cells as described by the manufacturer. All transfected cells were incubated at 37°C in 5% CO_2 for 8–24 h before microscopic imaging, unless otherwise noted.

Microscopy and image analysis

All fluorescence images were acquired with a laser-scanning confocal microscope (LSM-510; Carl Zeiss MicroImaging, Inc.) using either a 63× 1.4 NA Plan-Neofluar oil objective (Carl Zeiss MicroImaging, Inc.) or, for photoactivation and imaging of PEX16-PAGFP, a 40× 1.3 NA Plan-Neofluar oil objective (Carl Zeiss MicroImaging, Inc.). The imaging of GFP, PAGFP, Venus, and Cerulean was performed using 458-, 488-, and 514-nm lines of an argon ion laser (Lasos), and the imaging of RFP and Alexa Fluor 543 was performed using a 543 helium neon laser (Lasos). The dichroic mirrors used were 413/488, 458/514, and 488/543, with the appropriate filters supplied by the manufacturer (Carl Zeiss MicroImaging, Inc.) depending on the fluorophore and laser line. All cells were maintained at 37°C using an air blower.

For photo/pulse-chase experiments (Fig. 2) photoactivations of PAGFP were performed using a 413-nm laser (Coherent Enterprise II) at full power in a rectangular ROI. The ROI was selected in an area of the transformed cell that was free of peroxisomes as indicated by RFP-SKL. Photoactivations were repeated once every minute for a period of 30 min.

The de novo peroxiosme biogenesis assay (Fig. 7) was performed on NRK cells transfected with pPAGFP-SKL and pPEX16-Cerulean 12–15 h before photoactivation. The entire cell expressing PEX16-Cerulean was photoactivated using two iterations of a 413-nm laser line at full power in a rectangular ROI. Three z section images of 1 μm thickness were collected immediately before and after the photoactivation. 24 h after photoactivation, cells were fixed with 3.7% formaldehyde in phosphate-buffered saline for 15 min at room temperature before another round of photoactivation. Again, three z section images of the cell were collected immediately before and after the second photoactivation. Z sections were complied into one projection using the computer software Lview (Carl Zeiss MicroImaging, Inc.). ImageJ software (NIH) was used to calculate the number of peroxisomes in each cell. In brief, images were converted into threshold images that were then analyzed with the ImageJ "analyze particle" macro.

FLIP was performed using 25 iterations of a 488-nm laser at full strength in a rectangular ROI repeated every 90 s. An image was collected immediately before and after each photobleaching session. All images were adjusted for brightness and contrast using Photoshop CS (Adobe).

In vitro binding assay

In vitro transcription and translation reactions and the membrane binding assay were performed as described previously (Kim et al., 1997). Cotranslational targeting reactions were performed in the presence of 1 equivalence of ER microsomes (1 equivalence = 1 fmol of signal recognition particle receptor α-subunit (Walter and Blobel, 1983). Posttranslational reactions were stopped by adding cycloheximide to a final concentration of 20 μg/ml before adding 1 equivalence of ER microsomes. 1 h after incubation at 24°C, ER microsomes were separated from both cotranslational and posttranslational reactions by subjecting each reaction to centrifugation over a 0.5-M sucrose cushion. Equal amounts of each fraction were analyzed by SDS-PAGE using a Tris-Tricine buffer system (Schagger and von Jagow, 1987), and radioactive proteins were visualized and quantified using a phosphorimager (Typhoon; GE Healthcare).

Online supplemental material

Fig. S1 shows the relative expression of GFP-SKL, PEX16-GFP, and saPEX16-GFP over time. Fig. S2 shows the cellular localization of delPEX16-GFP before and after FLIP. Fig. S3 the differential cell permeabilization assay of cells expressing ssGFP-KDEL, PEX16-GFP, and saPEX16-GFP. Fig. S4 shows cellular localization of PEX3- and PMP34-GFP and the colocalization of PEX3-Cerulean with PEX16-Venus in PBD399-T1 cells. Online supplemental material is available at http://www.jcb.org/cgi/content/full/jcb.200601036/DC1.

The authors would like to thank Ramanujan Hegde, Erik Snapp, Sandra Kim, Jennifer Gillette, Carolyn Ott, John Dyer, and members of our laboratories for critical reading of the manuscript.

This work was supported by grants from National Institutes of Health to J. Lippincott-Schwartz and the Natural Sciences and Engineering Research Council of Canada to R.T. Mullen. R.T. Mullen holds the Ontario Premier's Research in Excellence Award.

Submitted: 9 January 2006
Accepted: 18 April 2006

References

Andrews, D.W., L. Lauffer, P. Walter, and V.R. Lingappa. 1989. Evidence for a two-step mechanism involved in assembly of functional signal recognition particle receptor. *J. Cell Biol.* 108:797–810.

Brocard, C.B., K.K. Boucher, C. Jedeszko, P.K. Kim, and P.A. Walton. 2005. Requirement for microtubules and dynein motors in the earliest stages of peroxisome biogenesis. *Traffic.* 6:386–395.

Eitzen, G.A., R.K. Szilard, and R.A. Rachubinski. 1997. *J. Cell Biol.* 137:1265–1278.

Fang, Y., J.C. Morrell, J.M. Jones, and S.J. Gould. 2004. PEX3 functions as a PEX19 docking factor in the import of class I peroxisomal membrane proteins. *J. Cell Biol.* 164:863–875.

Gafvelin, G., M. Sakaguchi, H. Andersson, and G. von Heijne. 1997. Topological rules for membrane protein assembly in eukaryotic cells. *J. Biol. Chem.* 272:6119–6127.

Geuze, H.J., J.L. Murk, A.K. Stroobants, J.M. Griffith, M.J. Kleijmeer, A.J. Koster, A.J. Verkleij, B. Distel, and H.F. Tabak. 2003. Involvement of the endoplasmic reticulum in peroxisome formation. *Mol. Biol. Cell.* 14:2900–2907.

Guo, T., Y.Y. Kit, J.-M. Nicaud, M.-T. Le Dall, S.K. Sears, H. Vali, H. Chan, R.A. Rachubinski, and V.I. Titorenko. 2003. Peroxisome division in the yeast *Yarrowia lipolytica* is regulated by a signal from inside the peroxisome. *J. Cell Biol.* 162:1255–1266.

Heiland, I., and R. Erdmann. 2005. Biogenesis of peroxisomes. Topogenesis of the peroxisomal membrane and matrix proteins. *FEBS J.* 272:2362–2372.

Heinrich, S.U., W. Mothes, J. Brunner, and T.A. Rapoport. 2000. The Sec61p complex mediates the integration of a membrane protein by allowing lipid partitioning of the transmembrane domain. *Cell.* 102:233–244.

Hoepfner, D., D. Schildknegt, I. Braakman, P. Philippsen, and H.F. Tabak. 2005. Contribution of the endoplasmic reticulum to peroxisome formation. *Cell.* 122:85–95.

Honsho, M., T. Hiroshige, and Y. Fujiki. 2002. The membrane biogenesis peroxin Pex16p. Topogenesis and functional roles in peroxisomal membrane assembly. *J. Biol. Chem.* 277:44513–44524.

Hunt, J.E., and R.N. Trelease. 2004. Sorting pathway and molecular targeting signals for the *Arabidopsis* peroxin 3. *Biochem. Biophys. Res. Commun.* 314:586–596.

Jones, J.M., J.C. Morrell, and S.J. Gould. 2004. PEX19 is a predominantly cytosolic chaperone and import receptor for class 1 peroxisomal membrane proteins. *J. Cell Biol.* 164:57–67.

Karnik, S.K., and R.N. Trelease. 2005. *Arabidopsis* peroxin 16 coexists at steady state in peroxisomes and endoplasmic reticulum. *Plant Physiol.* 138:1967–1981.

Kim, P.K., F. Janiak-Spens, W.S. Trimble, B. Leber, and D.W. Andrews. 1997. Evidence for multiple mechanisms for membrane binding and integration via carboxyl-terminal insertion sequences. *Biochemistry.* 36:8873–8882.

Koch, A., G. Schneider, G.H. Luers, and M. Schrader. 2004. Peroxisome elongation and constriction but not fission can occur independently of dynamin-like protein 1. *J. Cell Sci.* 117:3995–4006.

Kragt, A., T. Voorn-Brouwer, M. van den Berg, and B. Distel. 2005. Endoplasmic reticulum-directed Pex3p routes to peroxisomes and restores peroxisome formation in a *Saccharomyces cerevisiae* pex3Δ strain. *J. Biol. Chem.* 280:34350–34357.

Kunau, W.H. 2005. Peroxisome biogenesis: end of the debate. *Curr. Biol.* 15:R774–R776.

Lazarow, P.B. 2003. Peroxisome biogenesis: advances and conundrums. *Curr. Opin. Cell Biol.* 15:489–497.

Lazarow, P.B., and Y. Fujiki. 1985. Biogenesis of peroxisomes. *Annu. Rev. Cell Biol.* 1:489–530.

Mullen, R.T., C.S. Lisenbee, J.A. Miernyk, and R.N. Trelease. 1999. Peroxisomal membrane ascorbate peroxidase is sorted to a membranous network that resembles a subdomain of the endoplasmic reticulum. *Plant Cell.* 11:2167–2185.

Nagai, T., K. Ibata, E.S. Park, M. Kubota, K. Mikoshiba, and A. Miyawaki. 2002. A variant of yellow fluorescent protein with fast and efficient maturation for cell-biological applications. *Nat. Biotechnol.* 20:87–90.

Novikoff, A.B., and E. Holtzman. (1976) Cells and Organelles. 2nd ed. Holt, Rinehart and Winston, New York. 400 pp.

Patterson, G.H., and J. Lippincott-Schwartz. 2002. A photoactivatable GFP for selective photolabeling of proteins and cells. *Science.* 297:1873–1877.

Pedrazzini, E., A. Villa, R. Longhi, A. Bulbarelli, and N. Borgese. 2000. Mechanism of residence of cytochrome b_5, a tail-anchored protein, in the endoplasmic reticulum. *J. Cell Biol.* 148:899–914.

Rapoport, T.A., B. Jungnickel, and U. Kutay. 1996. Protein transport across the eukaryotic endoplasmic reticulum and bacterial inner membranes. *Annu. Rev. Biochem.* 65:271–303.

Rizzo, M.A., G.H. Springer, B. Granada, and D.W. Piston. 2004. An improved cyan fluorescent protein variant useful for FRET. *Nat. Biotechnol.* 22:445–449.

Sacksteder, K.A., J.M. Jones, S.T. South, X. Li, Y. Liu, and S.J. Gould. 2000. PEX19 binds multiple peroxisomal membrane proteins, is predominantly cytoplasmic, and is required for peroxisome membrane synthesis. *J. Cell Biol.* 148:931–944.

Schagger, H., and G. von Jagow. 1987. Tricine-sodium dodecyl sulfate-polyacrylamide gel electrophoresis for the separation of proteins in the range from 1 to 100 kDa. *Anal. Biochem.* 166:368–379.

Schekman, R. 2005. Peroxisomes: another branch of the secretory pathway? *Cell.* 122:1–2.

Schliebs, W., and W.H. Kunau. 2004. Peroxisome membrane biogenesis: the stage is set. *Curr. Biol.* 14:R397–R399.

South, S.T., and S.J. Gould. 1999. Peroxisome synthesis in the absence of pre-existing peroxisomes. *J. Cell Biol.* 144:255–266.

South, S.T., K.A. Sacksteder, X. Li, Y. Liu, and S.J. Gould. 2000. Inhibitors of COPI and COPII do not block PEX3-mediated peroxisome synthesis. *J. Cell Biol.* 149:1345–1360.

Tam, Y.Y., A. Fagarasanu, M. Fagarasanu, and R.A. Rachubinski. 2005. Pex3p initiates the formation of a preperoxisomal compartment from a subdomain of the endoplasmic reticulum in *Saccharomyces cerevisiae*. *J. Biol. Chem.* 280:34933–34939.

Titorenko, V.I., and R.A. Rachubinski. 1998. The endoplasmic reticulum plays an essential role in peroxisome biogenesis. *Trends Biochem. Sci.* 23:231–233.

Visser, W.F., C.W. van Roermund, H.R. Waterham, and R.J. Wanders. 2002. Identification of human PMP34 as a peroxisomal ATP transporter. *Biochem. Biophys. Res. Commun.* 299:494–497.

Veenhuis, M., F.A. Salomons, and I.J. Van Der Klei. 2000. Peroxisome biogenesis and degradation in yeast: a structure/function analysis. *Microsc. Res. Tech.* 51:584–600.

Walter, P., and G. Blobel. 1983. Signal recognition particle: a ribonucleoprotein required for cotranslational translocation of proteins, isolation and properties. *Methods Enzymol.* 96:682–691.

Wanders, R.J. 2004. Metabolic and molecular basis of peroxisomal disorders: a review. *Am. J. Med. Genet. A.* 126:355–375.

Yan, M., N. Rayapuram, and S. Subramani. 2005. The control of peroxisome number and size during division and proliferation. *Curr. Opin. Cell Biol.* 17:376–383.